

# A No-Reference Objective Image Sharpness Metric Based on the Notion of Just Noticeable Blur (JNB)

Rony Ferzli and Lina J. Karam, *Senior Member, IEEE*

**Abstract**—This work presents a perceptual-based no-reference objective image sharpness/blurriness metric by integrating the concept of just noticeable blur into a probability summation model. Unlike existing objective no-reference image sharpness/blurriness metrics, the proposed metric is able to predict the relative amount of blurriness in images with different content. Results are provided to illustrate the performance of the proposed perceptual-based sharpness metric. These results show that the proposed sharpness metric correlates well with the perceived sharpness being able to predict with high accuracy the relative amount of blurriness in images with different content.

**Index Terms**—HVS, image assessment, image quality, no-reference, objective, perception, sharpness metric.

## I. INTRODUCTION

HERE has been an increasing need to develop quality measurement techniques that can predict perceived image/video quality automatically. These methods are useful in various image/video processing applications, such as compression, communication, printing, display, analysis, registration, restoration, and enhancement [1]. For example, a noise metric [2] can be used to estimate the quantization error caused by compression without accessing the original pictures, while a sharpness metric can be used as a control parameter for sharpness enhancement algorithms applied to digital imagery; a sharpness metric can also be used to estimate the blur caused by image compression algorithms.

Subjective quality metrics are considered to give the most reliable results since, for many applications, it is the end user who is judging the quality of the output. A subjective quality metric can be computed by preparing the test images, selecting an appropriate number of individuals, and asking their opinion based on specified criteria and conditions. Subjective quality metrics are costly, time-consuming and impractical for real-time implementation and system integration. On the other hand, objective metrics can be divided into three categories: full-reference, reduced-reference, and no-reference. In the former case, a processed image is compared to a reference such as the original image. For the reduced-reference case, only partial information

Manuscript received May 21, 2007; revised October 11, 2008. Current version published March 13, 2009. The associate editor coordinating the review of this manuscript and approving it for publication was Dr. Gaurav Sharma.

The authors are with the Department of Electrical Engineering, Arizona State University, Tempe, AZ 85287-5706 USA (e-mail: rony.ferzli@asu.edu; karam@asu.edu).

Color versions of one or more of the figures in this paper are available online at <http://ieeexplore.ieee.org>.

Digital Object Identifier 10.1109/TIP.2008.2011760

about the original image is available and described by a set of local features. In the latter case, the metric is not relative to a reference image, but rather an absolute value is computed based on some characteristics of the given image. Quality assessment without a reference is a challenging task; distinction between image features and impairments is often ambiguous.

Of particular interest to this work is the no-reference sharpness/blurriness objective metric. Note that blur in an image is due to the attenuation of the high spatial frequencies, which commonly occurs during filtering or visual data compression. The image blurriness metric can also be used to measure sharpness since blurriness and sharpness are inversely proportional. Sharpness metrics can also be combined with other metrics to assess the overall quality. Several no-reference objective sharpness metrics were proposed in the literature and are analyzed in [3].

In this paper, a new perceptual no-reference image sharpness metric based on the notion of just noticeable blur (JNB) is introduced. In this work, it is shown that the HVS will mask blurriness around an edge up to a certain threshold; we refer to this threshold as the JNB. Knowing that the HVS tolerance is subject-dependent, subjective testing is performed and the JNBs are determined in function of the local contrast and are used to derive an edge-based sharpness metric based on a HVS model that makes use of probability summation over space [4].

This paper is organized as follows. Section II presents an overview of existing no-reference objective image sharpness metrics. Section III presents a motivation for the need of an HVS-based image blur/sharpness metric, and presents the results of available no-reference sharpness metrics when applied to images having different levels of blurriness and with different content. Section IV describes the proposed sharpness metric including the derived HVS-based blur perception model based on the JNB concept and probability summation over space. Performance results are presented in Section V. A conclusion is given in Section VI.

## II. EXISTING NO-REFERENCE SHARPNESS METRICS: AN OVERVIEW

This section presents an overview of existing popular no-reference sharpness metrics. These include several categories starting by pixel-based techniques and including analysis of statistical properties and correlation between pixels. Transform-based approaches are also extensively used taking advantage of the fact that sharper edges increase the high frequency components. In addition, techniques based on image gradient and Laplacian, and which detect the slope of the edges in an image, are presented. Less popular techniques based on

histogram are also reported. Thirteen objective no-reference metrics are described as follows.

- Variance metric [5]: Calculated as the variance of the whole image; as the blurriness of the image increases, the edges are smoothed and the transitions between the grayscale levels in the image decrease; thus, the variance decreases.
- Autocorrelation-based metric [6]: Derived from the auto-correlation function which uses the difference between auto-correlation values at two different distances along the horizontal and vertical directions, respectively. If the image is blurred or the edges are smoothed, the correlation between neighboring pixels becomes high. Consequently, the autocorrelation will increase and, thus, the sum of the difference metric will decrease.
- Derivative-based metrics [6]: Include the first-order (gradient) and second-order (Laplacian) derivatives metrics. These metrics act as a high-pass filter in the frequency domain. While the Laplacian-based method has good accuracy, it is highly sensitive to noise. For derivative-based methods, the higher the metric, the sharper the image is.
- Perceptual blur metric [7]: Proposed by Marziliano *et al.* to measure image blurriness. Edge detection is applied first and then, each row of the image is scanned to locate edge pixels; the start and end positions of the edge are defined as the locations of local extrema closest to edge. The edge width is calculated as the distance between the end and start positions. The overall metric is calculated as the average of the edge widths of the local blur values over all edges found. The sharper the image, the lower the metric is.
- Frequency threshold metric [8]: Based on computing the summation of all frequency component magnitudes above a certain threshold  $\Omega$ . The threshold is chosen experimentally and it is usually set between  $[\pi/4, \pi/2]$ . By increasing the threshold, we may catch more edges but, at the same time, the metric will be more susceptible to noise. Again, the sharper the image, the higher the metric is.
- Kurtosis metric [9], [10]: The kurtosis is a statistical measure of the peakedness or flatness of a distribution; a narrow distribution has high kurtosis and vice versa. It can be used in the frequency domain for measuring sharpness. Zhang *et al.* [9] show that the spectral density function can be considered as a 2-D probability density function of a bivariate random vector. Increasing the image sharpness will decrease the kurtosis; blurring the image will increase the kurtosis. So, the kurtosis is inversely proportional to the sharpness.
- Histogram threshold metric [8]: Defined as the weighted sum of the histogram bins values above a certain threshold “T.” The weights are considered to be the gray levels themselves. The threshold, “T,” is selected usually to be near the mean of the image. It is assumed that a sharper image contains a higher number of grayscale levels and, thus, the histogram will be wider containing a higher number of bins. The sharper the image, the higher the metric is.
- Histogram entropy-based metric [11]: The entropy is a measure of the information content of an image; if the probability of occurrence of each gray level is low, the entropy is high and vice versa. The probabilities are calculated by normalizing the obtained histogram. Sharper im-

ages contain a larger number of gray levels, meaning a lower probability and, thus, higher entropy.

- Histogram frequency-based metric [12]: The metric proposed by Marichal *et al.* is based on the occurrence histogram of nonzero DCT coefficients throughout all  $8 \times 8$  blocks of the image (more weight is given to DCT coefficients on the diagonal). The blurriness metric is estimated by examining the number of coefficients that are almost always zero by counting the number of zeros in the histogram. Note that the metric is lower for sharper images.
- Shaked-Tastl metric [13]: The metric is based on the high-pass to band-pass frequency ratio applied to local features that are extracted by thresholding the bandpass filter output. The sharper the image the higher the ratio since the number of high frequency components in the spectrum increases resulting in higher energy at the output of the highpass filter.
- Image Quality Measure (IQM) metric [14]: The metric calculates the normalized image power spectrum weighted by a modulation transfer function (MTF). The MTF is derived empirically taking into account the response of the Human Visual System to different image frequencies (i.e., cycles/deg) [15], [16]. The higher the metric, the sharper the image is.
- Noise Immune Sharpness (NIS) metric [3]: Relies on the Lipschitz regularity properties separating the signal singularities from the noise singularities, by applying the dyadic wavelet transform and then measuring the sharpness using the perceptual blur metric [7]. In contrast to other existing sharpness metrics, this metric will perform well under low to moderate SNR since the noise will be reduced across wavelet scales. The sharper the image, the lower the metric is.
- No-reference Blur metric [17]: This metric first finds the edge pixels using the Canny edge detector. For each edge pixel, the local extrema (i.e., minimum and maximum), along the gradient direction and closest to the edge pixel, are located and the edge width is calculated by counting the number of pixels with increasing grayscale values from one side and the number of pixels with decreasing grayscale values from the other side. The average edge widths over all the pixels is then found and used in an exponential model to find the quality metric. Note that the parameters of the exponential model need to be estimated by performing a training over a large data set of images with available subjective ratings. The sharper the image, the lower the metric is.

Most of the aforementioned existing metrics were mainly developed for “auto-focus” applications, where the primary requirement is to ensure the monotonicity of the perceived blur with the metric for a single image.

### III. EXISTING NO-REFERENCE SHARPNESS METRICS: PRELIMINARY EVALUATION

This section describes the initial testing bed used to evaluate the performance of the sharpness metrics presented in Section II. The obtained performance results are also reported in this section. A more thorough evaluation of these metrics is presented in Section V, where they are also compared to the proposed sharpness metric.

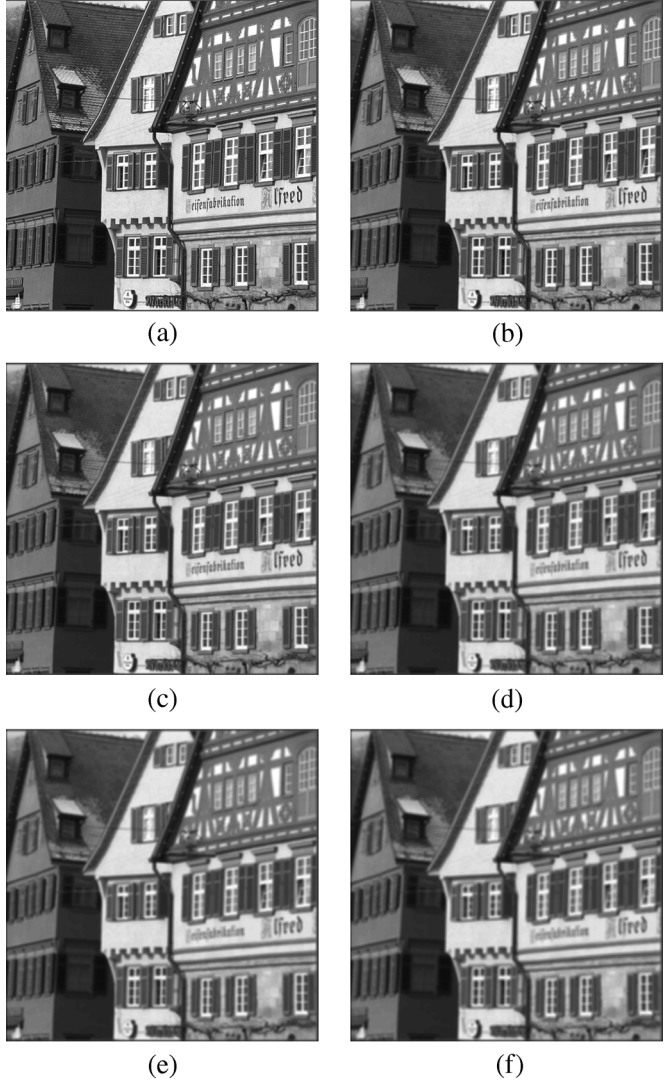


Fig. 1. Testing images for Set 1. (a) Original image; (b) blurred image ( $\sigma_{\text{blur}} = 0.8$ ); (c) blurred image ( $\sigma_{\text{blur}} = 1.2$ ); (d) blurred image ( $\sigma_{\text{blur}} = 1.6$ ); (e) blurred image ( $\sigma_{\text{blur}} = 2.0$ ); (f) blurred image ( $\sigma_{\text{blur}} = 2.4$ ).

#### A. Testing Sets

The testing sets consist of the following.

- Set 1: This testing set consists of a  $512 \times 512$  Houses image having different blur amounts. Different blur amounts were obtained by filtering the image using a  $7 \times 7$  Gaussian filter with a standard deviation equal to 0.8, 1.2, 1.6, 2.0, and 2.4, respectively. Fig. 1 shows the original and the blurred versions of the  $512 \times 512$  Houses image.
- Set 2: This testing set consists of four  $512 \times 512$  different images blurred using a  $7 \times 7$  Gaussian filter with a standard deviation equal to 0.8, 1.6, 2.0, and 2.4, respectively, as shown in Fig. 2.

#### B. Performance Evaluation

Note that, for all described metrics, as the blurriness of the images increases, the metric is expected to decrease except for the perceptual blur [7], kurtosis-based metrics [9], [10],

and the no-reference blur metric [17]. So, the multiplicative inverse of these metrics is calculated and used for assessing the image sharpness. Table I summarizes the performance results obtained for the different sharpness metrics that are described in Section II, when applied to Sets 1 and 2. The simulation results reveal that the metrics decrease monotonically as expected when applied to identical images (having same content) with increasing blurriness amounts (Set 1) except for the histogram threshold metric. This metric sometimes fails due to the fact that sharper images may not always result in a wider histogram.

All the metrics fail under test Set 2; no metric could differentiate between blurriness of these different images. The failure of the metrics can be due to the difference in the local image characteristics including intensity, frequency, and contrast. For example, from Fig. 2, it can be seen that the “Peppers” image contains smooth regions, the “Man” image has a considerable amount of texture, while sharp edges can be found in the “Fishingboat” and “Houses” images. As indicated in Section II, several of the existing blur metrics were not intended to be used across images with diverse content but were mainly developed to assess the blur in blurred versions of a single image.

This work focuses on automatically measuring the sharpness/blurriness across images with different contexts (Set 2). As shown in Table II, all existing metrics fail to predict the increase in blurriness across images with different contexts (Set 2). Since all existing no-reference metrics failed to predict correctly the relative blurriness for Set 2, an initial subjective testing was conducted, in order to check whether the difference in blurriness across these images can or cannot be perceived by the HVS. The subjective experiments followed the ITUT-R BT.500-10 recommendation [18] with the following conditions.

- 1) Subjects were given a set of instructions before starting such as how to conduct the experiments, and what is the objective of the experiment.
- 2) Experiments are conducted using a 21" CRT SUN monitor having a resolution of  $1280 \times 1024$ .
- 3) From time to time, the screen is grayed to avoid the effect of persistence.

Four subjects, with no image processing experience and with normal or corrected-to-normal vision, participated in the experiment. The subjects had to compare pairs of images taken from Set 2, in each of 6 different combinations as shown in Table III, and they had to state, for each pair, which of the two images is more blurred. Note that the sequence of displayed combinations is random. Results reveal that the subjects were able to differentiate the level of blurriness between different images, even when the blurriness amount difference is small, while none of the existing metrics did. So, there is a need to develop a reliable HVS-based blur/sharpness metric that can predict the perceived sharpness. For this purpose, as described below in Section IV, we study the behavior of the HVS when exposed to different levels of blurriness and derive an HVS-based blur/sharpness perception model that can be incorporated within a no-reference blur/sharpness metric.

#### IV. PROPOSED NO-REFERENCE SHARPNESS METRIC

The proposed no-reference objective sharpness metric integrates the concept of JNB into a probability summation model,



Fig. 2. Testing images for Set 2. (a) “Fishingboat” ( $\sigma_{\text{blur}} = 0.8$ ); (b) “Man” image ( $\sigma_{\text{blur}} = 1.6$ ); (c) “Peppers” image ( $\sigma_{\text{blur}} = 2.0$ ); (d) “Houses” image ( $\sigma_{\text{blur}} = 2.4$ ).

TABLE I  
PERFORMANCE OF EXISTING NO-REFERENCE SHARPNESS METRICS

	Set 1	Set 2
Variance [5]	yes	no
Autocorrelation based+ [6]	yes	no
Gradient [6]	yes	no
Laplacian [6]	yes	no
Perceptual Blur [7]	yes	no
Frequency threshold+ [8]	yes	no
Kurtosis [9], [10]	yes	no
Histogram threshold+ [8]	no	no
Histogram entropy based [11]	yes	no
Histogram frequency based [12]	yes	no
Shaked-Tastl [13]	yes	no
IQM [14]	yes	no
NIS [3]	yes	no
Blur Reference Metric [17]	yes	no
yes = Metric decreasing monotonically for the considered Set		
no = Metric failing to decrease monotonically for the considered Set		

resulting in a distortion metric that can predict the relative blurriness in images based on the probability of blur detection. The JNB concept and the blur detection model based on probability summation are first described in Sections IV-A and IV-B, respectively, followed by a description of the proposed no-reference sharpness metric in Section IV-C.

#### A. Just Noticeable Blur (JNB) Concept

A great deal of research has been done in the field of image and video quality analysis using algorithms which simulate the Human Visual System. Most of these algorithms are based on the notion of “just noticeable difference” (JND) [19]. By definition, the JND is the minimum amount by which a stimulus intensity must be changed relative to a background intensity in order to produce a noticeable variation in sensory experience. In other words, the required difference such that the standard observer can detect a change of intensity [20]. Contrast is a key concept in vision science because the information in the visual system is represented in terms of contrast and not in terms of

TABLE II  
RESULTS FOR DIFFERENT NO-REFERENCE METRICS APPLIED TO SET 2

Metrics	Blur Variance			
	0.8	1.6	2.0	2.4
Variance [5]	0.67	0.98	0.88	1.00
Autocorrelation Based [6]	0.99	1.00	0.59	0.82
Gradient [6]	0.73	0.74	0.59	1.00
Laplacian [6]	1.00	0.21	0.14	0.28
Perceptual blur [7]	1.0	0.50	0.30	0.61
Frequency Threshold [8]	1.00	0.85	0.71	0.97
Kurtosis [9], [10]	0.12	0.09	1.00	0.45
Histogram threshold [8]	0.12	0.09	1.00	0.45
Histogram entropy based [11]	0.94	0.99	0.99	1.00
Histogram frequency based [12]	0.82	0.94	1.00	0.97
Shaked-Tastl [13]	1.00	0.64	0.41	0.55
IQM [14]	0.57	1.00	0.68	0.78
NIS [3]	0.37	0.64	1.00	0.59
No-Reference Blur Metric [17]	0.74	0.89	1.00	0.92

TABLE III  
IMAGE DISPLAY COMBINATION FOR SUBJECTIVE TESTING

Left Side	Right Side
Houses $\sigma = 2.4$	FishingBoat $\sigma = 0.8$
Man $\sigma = 1.6$	Peppers $\sigma = 2.0$
FishingBoat $\sigma = 0.8$	Man $\sigma = 1.6$
Peppers $\sigma = 2.0$	FishingBoat $\sigma = 0.8$
Man $\sigma = 1.6$	Houses $\sigma = 2.4$
Peppers $\sigma = 2.0$	Houses $\sigma = 2.4$

the absolute level of light; so, relative changes in luminance are important rather than absolute ones.

The “just noticeable blur” (JNB) is the minimum amount of perceived blurriness around an edge given a contrast higher than the JND. In order to study the response of the HVS to blurriness in images, subjective experiments were performed to obtain results in relation to blur perception and just-noticeable blurs (JNBs). The purpose is to estimate the maximum amount

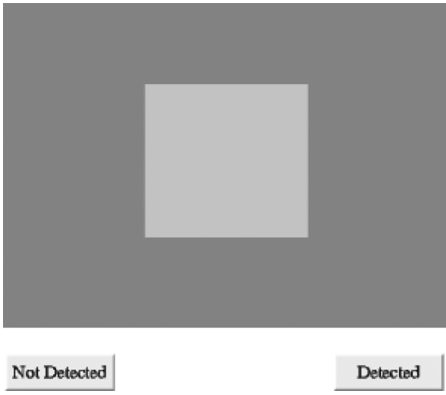
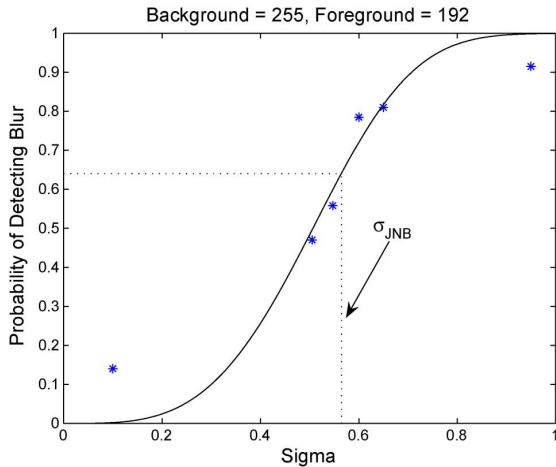


Fig. 3. Snapshot of the subjective test experiment.

Fig. 4. Example of nonlinear fitting to obtain  $\sigma_{JNB}$  for background and foreground intensities equal to 255 and 192, respectively.

of blurriness that can be introduced around an edge at a specific contrast without being perceived by the subjects.

For a given background intensity  $I_B$ , a rectangle with an intensity  $I_F$  is overlaid as the foreground, where  $I_F$  is chosen such that  $C = |I_F - I_B|$  is greater than the JND. The rectangular shape is chosen to analyze the blurriness effect around horizontal and vertical edges which are commonly found in natural images. For a given contrast  $C$ , the foreground square is blurred using a lowpass  $7 \times 7$  Gaussian mask with a standard deviation  $\sigma$  ranging from 0.1 to 0.95. The standard deviation values of the Gaussian filter are selected based on the preliminary experiments conducted by the authors in [21] where the subjects can increase the Gaussian mask variance until detecting blurriness labeled as JNB. In the following discussion, the notation  $\sigma_{JNB}$  is used to refer to the standard deviations of the Gaussian mask corresponding to the JNB thresholds.

In order to obtain the  $\sigma_{JNB}$  values, the following subjective test procedure is adopted.

- Background and foreground intensities,  $I_B$  and  $I_F$  can take any of the following grayscale values  $\{0, 30, 60, 80, 128, 192, 255\}$ ; cases where background and foreground have the same intensity are excluded. The grayscale values are limited in order to reduce the length of the subjective test.

TABLE IV  
MEASURED  $\sigma_{JNB}$  AND  $w_{JNB}$  FOR DIFFERENT CONTRASTS

Contrast = $ foreground - background $	$\sigma_{JNB}$	$w_{JNB}$
20	0.86	5
30	0.848	5
50	0.818	5
64	0.578	3
128	0.448	3
192	0.345	3
255	0.305	3

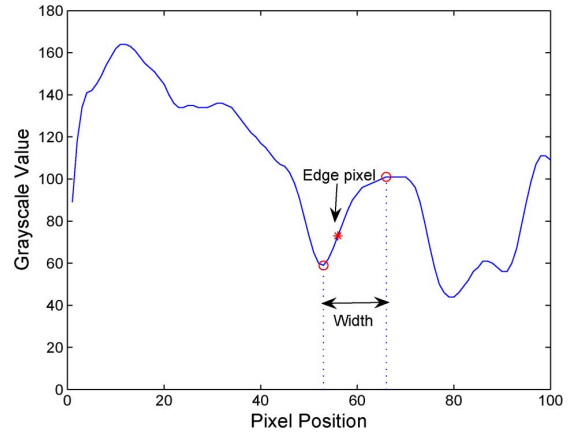


Fig. 5. Image horizontal line cut illustrating the measurement of the width around and edge pixel.

- To reduce the number of cases and, thus, the test duration, for each combination of background and foreground, six different Gaussian filters with different standard deviations are applied. Note that the six selected standard deviation values are different from one combination of foreground and background to the other but are all selected ranging between 0.1 and 0.95. Two out of the 6 standard deviation values are selected at the extremes (i.e.,  $\sigma = 0.1$  and  $\sigma = 0.95$ ) while the remaining four values are selected within the vicinity of what is believed to be the  $\sigma_{JNB}$  based on the preliminary tests conducted in [21].
- Each background, foreground and  $\sigma$  value combination is repeated 4 times for a better averaging of the subjective scores [22].
- The selection of the background and foreground intensities as well as the  $\sigma$  for the Gaussian filter is completely randomized.
- For each displayed combination, the user has to specify whether he/she detected blur or not. The subjects cannot control the amount of blurriness.

Fig. 3 shows a snapshot of the displayed interface for the conducted experiments. In the actual conducted experiments, the foreground square was of size  $256 \times 256$  and was located in the middle of the screen. The total number of subjects, who participated in these JNB experiments, was 18 with normal or corrected-to-normal vision. A 19" DELL UltraSharp 1905P LCD screen with a resolution of  $1280 \times 1024$  was used. Overall, the

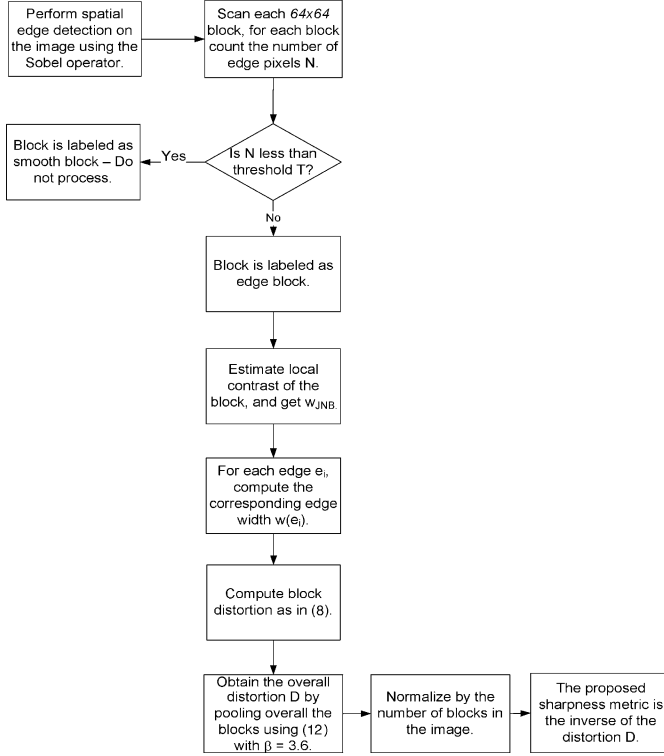


Fig. 6. Flowchart illustrating the computation of the proposed perceptual-based sharpness metric based on probability summation.

subject is exposed to 27 different contrasts  $C$  starting at 20 and reaching 255. For each contrast, the corresponding collected data is used to compute the  $\sigma_{\text{JNB}}$  threshold at the considered contrast. This is done by first computing, for each contrast  $C$ , the normalized histogram of the subjects' responses. The computed normalized histogram corresponds to the probability of detecting a blur distortion in function of the standard deviation  $\sigma$ . From the computed normalized histogram, the  $\sigma_{\text{JNB}}$  is selected to be the standard deviation corresponding to a probability of detection equal to 63% [23].

For a given contrast  $C$ , the probability of detecting a blur distortion takes the form of a psychometric function which is modeled as an exponential having the following form [4]:

$$P = 1 - \exp\left(-\left|\frac{\sigma}{\sigma_{\text{JNB}}}\right|^\beta\right) \quad (1)$$

where  $\sigma$  is the standard deviation of the Gaussian blur filter and corresponds to the blur strength at the considered edge, and  $\sigma_{\text{JNB}}$  is the standard deviation corresponding to the JNB threshold. From (1), note that a probability of detection of 63% is obtained when  $\sigma = \sigma_{\text{JNB}}$  as desired. In (1), the values of  $\beta$  and  $\sigma_{\text{JNB}}$  are chosen, by means of a least-square fitting, to increase the correspondence of (1) with the experimentally determined psychometric function (given by the normalized histogram of the subjects' responses). A fitting example for a background intensity of 255 and a foreground intensity of 192 is shown in Fig. 4. Table IV shows  $\sigma_{\text{JNB}}$  for different contrasts  $C$ . The obtained  $\beta$  values are between 3.4 and 3.8 with a median value of 3.6.

## B. Perceptual Blur Model Based on Probability Summation

While the derived JNB thresholds (Section IV-A) provide a localized measure of the blur threshold for a single edge at a given local contrast, a perceptual sharpness metric that also accounts for spatial summation of individual blur distortions is needed. In this work, the probability summation model is adopted [4]. The proposed probability summation model considers a set of independent detectors, one at each edge location  $e_i$ . The probability  $P(e_i)$  of detecting a blur distortion is the probability that a detector at edge pixel " $i$ " will signal the occurrence of a blur distortion.  $P(e_i)$  is determined by the psychometric function (1). The  $\sigma$  and  $\sigma_{\text{JNB}}$  in (1) can be replaced by their corresponding measured edge widths resulting in

$$P(e_i) = 1 - \exp\left(-\left|\frac{w(e_i)}{w_{\text{JNB}}(e_i)}\right|^\beta\right) \quad (2)$$

where  $w(e_i)$  is the measured width of the edge  $e_i$  and  $w_{\text{JNB}}(e_i)$  is the JNB width (Section IV-A) which depends on the local contrast in the neighborhood of edge  $e_i$ . For each blur detection threshold  $\sigma_{\text{JNB}}$ , the corresponding edge width is measured and denoted as  $w_{\text{JNB}}$ . The width around the edge is measured by counting the number of pixels with increasing grayscale values in one direction of the edge pixel while counting the number of pixels with decreasing grayscale values in the other direction. The width is then computed as the sum of both counts excluding the edge pixel. Note that the positive direction has the same direction as the gradient. Fig. 5 illustrates the width measurement by showing a row of an image with a detected edge pixel and corresponding width where local minima and maxima are shown and marked as "o." The  $w_{\text{JNB}}$  are measured to be 5 for  $C \leq 50$  and 3 for  $C \geq 51$ .

A less localized probability of error detection can be computed by adopting the "probability summation" hypothesis which pools the localized detection probabilities  $P(e_i)$  over a region of interest  $R$  [4]. The probability summation hypothesis is based on the following two assumptions.

- Assumption 1: A blur distortion is detected if and only if at least one detector in  $R$  senses the presence of a blur distortion.
- Assumption 2: The probabilities of detection  $P(e_i)$  are independent; i.e., the probability that a particular detector will signal the presence of a distortion is independent of the probability that any other detector will.

The probability of detecting blur in a region  $R$  is then given by

$$P_{\text{blur}}(R) = 1 - \prod_{e_i \in R} (1 - P(e_i)). \quad (3)$$

Substituting (2) into (3) yields

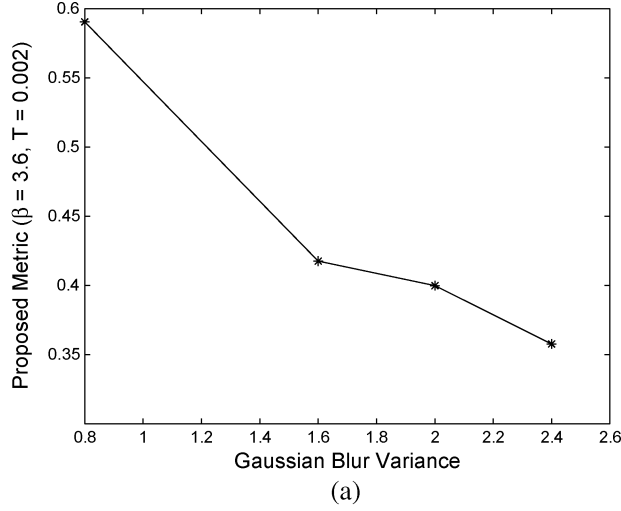
$$P_{\text{blur}}(R) = 1 - \exp\left(-D_{(R)}^\beta\right) \quad (4)$$

where

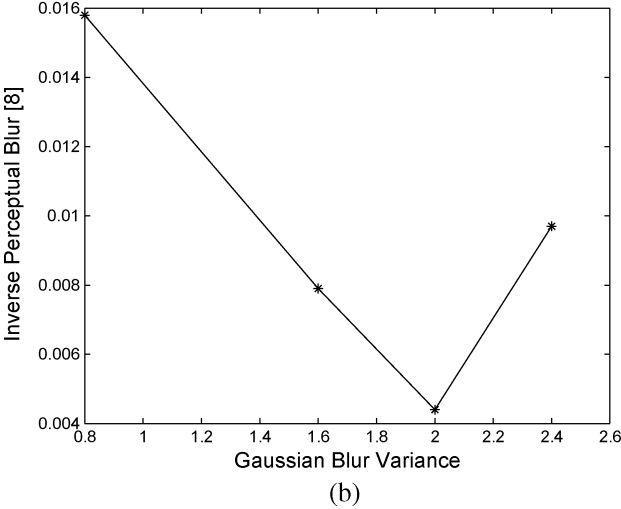
$$D_{(R)} = \left(\sum_{e_i \in R} \left|\frac{w(e_i)}{w_{\text{JNB}}(e_i)}\right|^\beta\right)^{\frac{1}{\beta}}. \quad (5)$$

TABLE V  
PROPOSED METRIC PERFORMANCE WHEN APPLIED TO SET 1

	Blur Variance					
	0	0.8	1.2	1.6	2.0	2.4
Proposed Metric Value	4.54	2.65	2.2	2.0	1.98	1.97



(a)



(b)

Fig. 7. Performance of the proposed perceptual-based sharpness metric and the perceptual blur metric of [7] when applied to the image testing Set 2. (a) Performance of the proposed metric when applied to Set 2. (b) performance of the perceptual blur metric [7] when applied to Set 2.

### C. Perceptual Sharpness Metric

The proposed perceptual sharpness metric will be based on the probability summation model presented in Section IV-B and will not be directly applied to the whole image, rather, the image will be divided into blocks. The block will be the region of interest  $R$ . The block size is chosen to correspond with the foveal region. Let  $r$  be the visual resolution of the display in pixels/degree,  $v$  the viewing distance in cm, and  $d$  the display resolution in pixels/cm. Then, the visual resolution  $r$  can be calculated as [24]

$$r = dv \tan\left(\frac{\pi}{180}\right) \approx d \frac{v\pi}{180} \approx d \frac{v}{57.3}. \quad (6)$$



(a)



(b)

Fig. 8. Sample Gaussian blurred images with different content. (a)  $640 \times 512$  “dancers” image ( $\sigma_{\text{blur}} = 1.47$ ); Perceptual blur metric [7] = 0.261; proposed metric value = 2.5213; MOS value from subjective testing = 3.04. (b)  $480 \times 512$  “woman” image ( $\sigma_{\text{blur}} = 0.648$ ); Perceptual blur metric [7] = 0.175, proposed metric value = 2.6387; MOS value from subjective testing = 4.88.

In the Human Visual System, the highest visual acuity is limited to the size of the foveal region, which covers approximately  $\alpha = 2^\circ$  of visual angle. Let  $F(n_1, n_2)$  denote the area in the spatial domain that is centered at location  $(n_1, n_2)$  and covers  $2^\circ$  of visual angle. The number of pixels contained in that region  $N$  can be computed as [24]

$$N(F(n_1, n_2)) = \left(2 \left[ dv \tan \frac{\alpha}{2} \right]\right)^2 \approx (2[r])^2 \quad (7)$$

where  $r$  is the display visual resolution (in pixels/degree) calculated in (6). Given a viewing distance  $v$  of 60 cm and 31.5 pixels-per-cm (80 pixels-per-inch) display results in a display visual resolution of 32.9 pixels/degree and  $N \approx (64)^2$ . In this

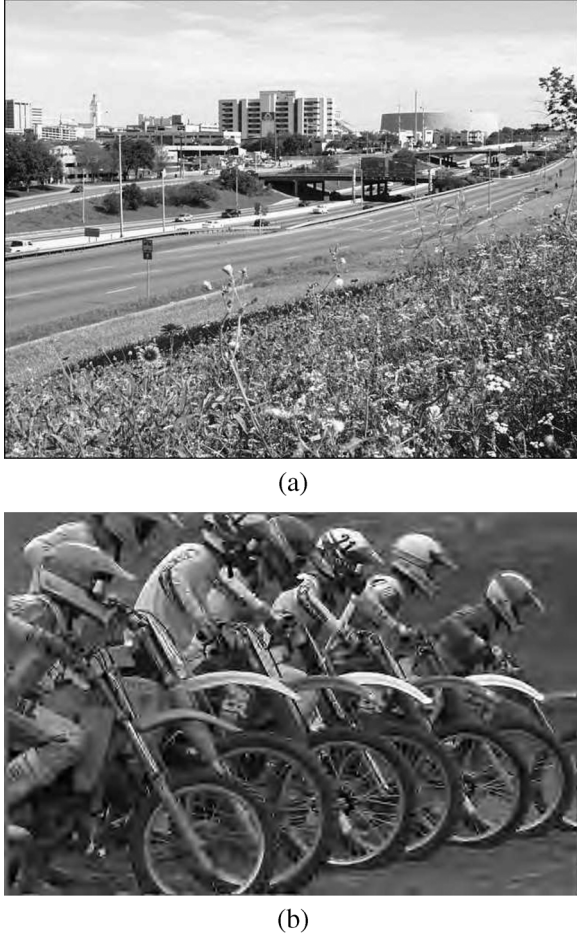


Fig. 9. Sample JPEG2000 blurred images with different content. (a) 640 × 512 “Flawsonih35” JPEG2000 image with a compression of 1.8386 bits/pixel, proposed metric value = 3.143, MOS = 4.5. (b) 768 × 512 “Bikes” JPEG2000 image with a compression of 0.13174 bits/pixel, proposed metric value = 1.517, MOS = 1.834.

work, the foveal region is approximated by an image block  $R$  of  $64 \times 64$ . Smooth blocks are excluded as they do not contribute to blur perception. For this purpose, a Sobel edge detector is run first on each block, and each block is categorized as a smooth block or an edge block. The decision is made based on the number of edge pixels in the block; if the number is higher than a threshold  $T$ , the block is considered an edge block; otherwise it is considered a smooth block. The threshold is chosen to be a percentage of the block. For a  $64 \times 64$  block, the threshold is chosen to be 0.2% of the total number of pixels in the block [25]. For each edge block, edge pixels are located and the corresponding width is computed. In the current implementation, only horizontal edges are detected as in [7]. The perceived blur distortion within an edge block  $R_b$  is given by

$$D_{R_b} = \left( \sum_{e_i \in R_b} \left| \frac{w(e_i)}{w_{\text{JNB}}(e_i)} \right|^{\beta} \right)^{\frac{1}{\beta}} \quad (8)$$

where  $w_{\text{JNB}}$  is the JNB width corresponding to the contrast of the considered block region  $R_b$  and is obtained as described in Section IV.

The perceived blur distortion measure  $D$  for the whole image  $I$  corresponds to the probability of detecting a blur distortion over all possible block regions  $R_b$  and is obtained by using a Minkowski metric for interblock pooling. The probability of detecting blur in the image  $I$  is, thus, given by

$$P_{\text{blur}}(I) = 1 - \prod_{R_b \in I} (1 - P_{\text{blur}}(R_b)) \quad (9)$$

where  $P_{\text{blur}}(R_b)$  can be written as in (4) to be

$$P_{\text{blur}}(R_b) = 1 - \exp(-D_{(R_b)}^{\beta}). \quad (10)$$

Substituting (10) into (9) yields

$$P_{\text{blur}}(I) = 1 - \exp(-D^{\beta}) \quad (11)$$

where

$$D = \left( \sum_{R_b} |D_{R_b}|^{\beta} \right)^{\frac{1}{\beta}}. \quad (12)$$

As indicated in Section IV-A,  $3.4 \leq \beta \leq 3.8$  with a median value of 3.6. However, it was found that fixing  $\beta$  to its median value of 3.6 in (12) results in a performance comparable to using a different value of  $\beta$  for each contrast  $C$ .

The resulting blur distortion measure  $D$  of (12), normalized by the total number of processed blocks (i.e., nonsmooth blocks) in an image, is adopted as the proposed no-reference objective blurriness metric. The proposed no-reference objective sharpness metric is, thus, given by

$$S = \left( \frac{L}{D} \right) \quad (13)$$

where  $L$  is the total number of processed blocks in the image and  $D$  is given by (12). A block diagram summarizing the computation of the proposed sharpness metric is given in Fig. 6.

## V. PERFORMANCE RESULTS

In this section, results are presented to illustrate the performance of the proposed JNB-based sharpness metric. For completeness, the proposed metric behavior is first presented for the image sets, Set 1 and Set 2, of Section III. Then, the performance of the proposed metric is tested using a variety of Gaussian-blurred and JPEG2000-compressed images from the LIVE database [26]. In order to validate the proposed objective no-reference metric, subjective tests were conducted for assessing the blur in different Gaussian-blurred and JPEG2000-compressed images from the LIVE database. Results are presented showing how well the proposed metric correlate with the subjective scores as compared to existing no-reference sharpness metrics.

### A. Performance Results Using Sets 1 and 2 (Section III)

Table V shows the obtained metric values when applied to Set 1, which consists of images having same content but different blur amounts as shown in Fig. 1. From Table V, it can



Fig. 10. Sample images with different sizes extracted from the LIVE Database for the subjective test; (a)–(c) Gaussian-blurred images, (d)–(f) JPEG2000 compressed images. (a) “Parrots” image,  $\sigma_{\text{blur}} = 7.6$ . (b) “Ocean” image,  $\sigma_{\text{blur}} = 5.8$ . (c) “Caps” image,  $\sigma_{\text{blur}} = 1.7$ . (d) “House” image, bit rate = 0.034 bits/pixel. (e) “Capitol” image, bit rate = 0.109 bits/pixel. (f) “Stream,” bit rate = 0.715 bits/pixel.

be seen that, as expected, the metric is decreasing monotonically as the blurriness increases. Fig. 7(a) illustrates the performance of the proposed perceptual-based sharpness metric when applied to the image testing Set 2. For comparison, Fig. 7(b) also shows the performance results when the popular nonperceptually weighted edge-based sharpness metric of Marziliano *et al.* [7] is applied to Set 2. Note that the sharpness metric of [7] is also referred to as the perceptual blur metric in the literature but it does not incorporate HVS-based perceptual weighting. Though other sharpness metrics exist as described in Section II, the blur perceptual metric of [7] is popular due to its simplicity, and is widely applied successfully to a broad range of images having same content but different blurriness levels [7]. Also, as indicated in Section II, all the existing sharpness metrics, including [7], fail to predict well the increase in blurriness in images with different content when tested on Set 2. This is further confirmed by the results in Fig. 7 which shows the obtained sharpness metric value as a function of the blur for Set 2. As the blurriness increases, the sharpness metric should decrease monotonically. From Fig. 7, it can be seen that the proposed perceptual JNB-based sharpness metric is decreasing as expected, while the perceptual blur metric of [7] is not. Ten subjects were also asked to rate the images at a scale of 1 to 5 going from a “Very Annoying” blur to “Imperceptible.” The obtained MOS for Figs. 2(a)–(d) are 4.1, 3.5, 3.3, and 2.9, respectively.

The following discussion focuses on performance results for a variety of images with different contexts since the focus of this work is on automatically measuring the sharpness/blurriness across images or subimages with different contexts (such as Set 2), which has various potential applications ranging from automatic quality (blur) control in a compression system or in a video/HDTV postprocessing chain to predicting the relative depth of different parts of an image, which is important for 3DTV applications, by applying the proposed metric to local regions or subimages within the image of interest.

### B. Performance Results for Gaussian-Blurred and JPEG2000-Compressed Images

The LIVE database was used for testing the performance of the proposed no-reference sharpness metric in addition to existing popular no-reference sharpness metrics [7], [17]. The LIVE database consists of 29 high-resolution 24-bits/pixel RGB color images (typically  $768 \times 512$ ). The images are distorted using different distortion types: JPEG2000, JPEG, white noise in the RGB components, Gaussian blur in the RGB components, and bit errors in the JPEG2000 bitstream when transmitted over a simulated fast-fading Rayleigh channel. The Gaussian-blurred images in the LIVE database are generated using a circular-symmetric 2-D Gaussian kernel of standard deviation  $\sigma_{\text{blur}}$  ranging from 0 to 15 while the JPEG2000-compressed images are generated by using a JPEG2000 software with a compression rate ranging from lossless to 0.05 bits/pixel. Performance results are presented here for both Gaussian- and JPEG2000-compressed images of the LIVE database.

Fig. 8(a) and (b) shows different Gaussian-blurred images from the LIVE database along with blur metric values corresponding to the proposed metric, the perceptual blur metric of [7], and MOS subjective ratings. It can be seen that, in contrast with the metric of [7], the proposed metric is following the perceived blurriness. Fig. 9(a) and (b) also shows different JPEG2000-compressed images from the LIVE database along with blur metric values corresponding to the proposed metric and MOS subjective ratings, indicating that the proposed metric is predicting correctly the JPEG2000 blur following the subjective rating.

In order to validate the proposed objective no-reference metric, subjective tests were conducted for assessing the blur in different images. Two tests were conducted, one using Gaussian-blurred images and the other using JPEG2000-compressed images. Both tests were conducted as follows.

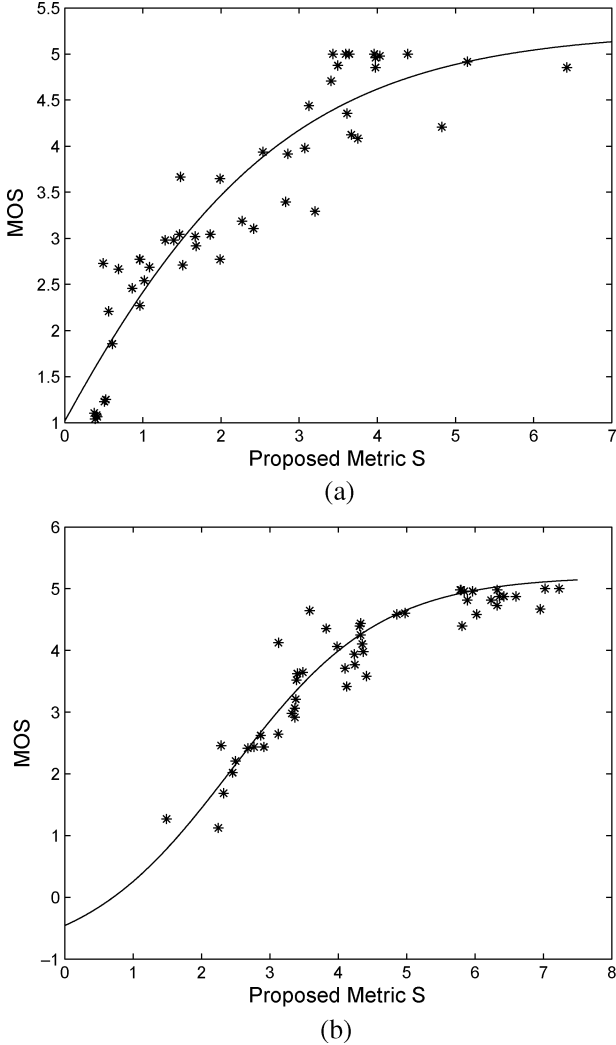


Fig. 11. Correlation of the proposed metric with the subjective tests. MOS computed from subjective tests and compared to the proposed metric values applied to the 50 images extracted from the LIVE database.  $\beta_1$ ,  $\beta_2$ ,  $\beta_3$  and  $\beta_4$  are the parameters of the logistic function. (a) Gaussian Blur,  $\beta_1 = 5.2499$ ,  $\beta_2 = -6.3354$ ,  $\beta_3 = -0.9588$ , and  $\beta_4 = 1.7367$ . (b) JPEG2000 Blur,  $\beta_1 = 5.2025$ ,  $\beta_2 = -1.0572$ ,  $\beta_3 = 2.4425$ , and  $\beta_4 = 1.0897$ .

- Fifty images are extracted from the LIVE database to be shown to the human observers (50 Gaussian-blurred and 50 JPEG2000-compressed images). In order to reduce the effect of subjects outliers [22], each image is presented 4 times giving a total of 200 Gaussian-blurred images and 200 JPEG2000-compressed images. A sample of these images is shown in Fig. 10.
- The images are randomly displayed; for each displayed image, the subject is asked to rate the quality of the image in terms of blurriness using a scale from 1 to 5 corresponding to “Very annoying,” “Annoying,” “Slightly annoying,” “Perceptible but not annoying,” and “Imperceptible,” respectively. Note that the subject cannot proceed to the next image unless the current image is scored.
- Twelve subjects took the test and the MOS is computed and compared to the proposed sharpness metric.

To measure how well the metric values correlate with the provided MOS values, the authors followed the suggestions of

the VQEG report [27] where several evaluation metrics are proposed. Note that a logistic fitting function is used, as suggested in [27], to provide a nonlinear mapping between the objective/subjective scores to accommodate for the quality rating compression at the extremes of the test range. The used logistic fitting function is given by

$$MOS_{p_i} = \frac{\beta_1 - \beta_2}{1 + e^{\left(\frac{metric_i - \beta_3}{|\beta_4|}\right)}} + \beta_2 \quad (14)$$

with  $\beta_1$ ,  $\beta_2$ ,  $\beta_3$ , and  $\beta_4$  are the model parameters,  $MOS_{p_i}$  is the predicted MOS, and  $metric_i$  is the proposed metric for image  $i$ . The fitted curves are shown in Fig. 11(a) and (b) for Gaussian-blurred and JPEG2000-compressed images, respectively.

Tables VI and VII show the evaluation results in terms of the Pearson (indicates the prediction accuracy), Spearman (indicates the prediction monotonicity), MAE (mean absolute prediction error) and OR (outlier ratio, indicates consistency) coefficients after nonlinear regression, for the Gaussian blur and JPEG2000 blur, respectively. Note that the Spearman rank-order correlation is nonparametric, where no assumptions are taken about the form of the relationship between the objective/subjective scores and, thus, the Spearman correlation is not affected by the nonlinear regression. From Table VI, it can be seen that, for the Gaussian-blurred images, the obtained Pearson and Spearman coefficients are above 0.9 indicating that the proposed metric is highly accurate, and monotonic [28]. In addition, the results in Table VI show the superiority of the proposed metric in terms of accuracy, monotonicity and consistency as compared to the existing metrics. The obtained outlier ratio (OR) for the proposed metric may be higher than expected but it is still lower than all the considered existing metrics. This is due to the fact that this ratio is a percentage of the number of prediction errors above a threshold which is taken to be twice the standard deviation of the subjects’ responses for each assessed image. This threshold is suggested in [27] assuming the subjects’ responses follow a Gaussian distribution which is not always the case in our collected data, especially when the subjective ratings are consistent resulting in a very small standard deviation.

From Table VI, it can be seen that the proposed metric as well as the metrics in [7], [17] outperform the other described ones, as such, only these three metrics are used to evaluate the performance for the JPEG2000-compressed images as shown in Table VII. Comparing Table VII to Table VI, it can be seen that the proposed metric correlates better with Gaussian blur since the JPEG2000-compressed images contain other types of distortions such as ringing affecting the visual assessment. From Table VII, it can be seen that the proposed metric exhibits significantly superior performance in terms of prediction accuracy and the monotonicity even for the JPEG2000-compressed images as indicated by the obtained Pearson and Spearman coefficients which are higher than the ones obtained for the existing metrics.

One drawback of the metric in [17] is that it requires training to a large image dataset to obtain the parameters of the exponential model  $\alpha + \beta s^\gamma$ , where  $s$  is measuring the average width around all edge pixels. In order to implement the metric of [17], for each type of blur (Gaussian and JPEG2000), half of the LIVE database was used for the training in order to obtain the

TABLE VI  
EVALUATION OF THE PROPOSED METRIC PERFORMANCE WHEN APPLIED TO GAUSSIAN BLUR

	Pearson (Non-linear Regression)	Spearman	MAE	RMS	OR
Proposed Metric	0.932	0.936	0.360	0.464	0.413
Marziliano et al. [7]	0.894	0.884	0.500	0.571	0.471
Ong et al. [17]	0.872	0.823	0.1563	13.60	11.2
Variance [5]	0.2848	0.3884	0.6	1.125	1.0619
Autocorrelation Based [6]	0.6584	0.872	0.74	1.274	1.12
Gradient [6]	0.785	0.777	0.52	0.789	0.6991
Laplacian [6]	0.5838	0.891	0.74	1.27	1.2
Frequency Threshold [8]	0.6906	0.7305	0.52	13.60	0.755
Kurtosis [9], [10]	0.72	0.75	0.56	0.88	0.81
Histogram threshold [8]	0.3037	0.2464	0.66	1.214	1.042
Histogram entropy based [11]	0.3675	0.3609	0.64	1.1851	1.0159
Histogram frequency based [12]	0.804	0.893	0.74	1.274	1.1204
Shaked-Tastl [13]	0.872	0.823	0.1563	13.60	11.2
IQM [14]	0.714	0.706	0.44	0.621	0.524
NIS [3]	0.732	0.754	0.52	0.786	0.802

TABLE VII  
EVALUATION OF THE PROPOSED METRIC PERFORMANCE WHEN APPLIED TO JPEG2000 BLUR

	Pearson (Non-linear Regression)	Spearman	MAE	RMS	OR
Proposed Metric	0.881	0.873	0.320	0.391	0.471
Marziliano et al. [7]	0.782	0.761	0.482	0.561	0.445
Ong et al. [17]	0.799	0.732	0.1367	14.80	12.3

model parameters of [17]; the other half was used for the testing. Eighty-four Gaussian-blurred images were used for training resulting in the parameters  $\alpha = -123.364$ ,  $\beta = 226.1236$ , and  $\gamma = 0.3541$  for the Gaussian blur. For the JPEG2000 blur, 110 JPEG2000-compressed images were used for training resulting in  $\alpha = -329.269$ ,  $\beta = 443.5947$ , and  $\gamma = 0.3073$ . Note that the raw score scale provided by the LIVE database is between 0 and 100 [26]. Note that the performance of the metric [17] is significantly lower than the proposed one.

## VI. CONCLUSION

A perceptual sharpness metric is derived based on measured just-noticeable blurs (JNBs) and probability summation over space, which takes into account the response of the HVS to sharpness at different contrast levels. Combining the derived model with local image features, it is shown that the proposed metric is able to successfully predict the relative sharpness/blurriness of images, including those with different scenes. Future directions of research include improving the performance of the proposed metric for very large blur values (e.g., Gaussian blur with a standard deviation greater than 8) since, in such cases, the proposed as well as the existing no-reference sharpness metrics tend to underestimate the amount of blurriness due to the fact that, at significantly high blur levels, many of the image details and edges are wiped out, which would affect the performance of the edge-based no-reference sharpness metrics. In addition,

future research will focus on enhancing the metric behavior in some corner cases. For example, if one considers only images with blurry backgrounds and with sharp foregrounds having regions that attract human visual attention (such as faces), the correlations of the proposed and existing no-reference sharpness metrics with subjective scores decline showing the need to integrate a visual attention model within these metrics. Other future directions of research include investigating the effect of color on sharpness perception and incorporating the proposed JNB concept into a noise-immune sharpness metric [3].

## REFERENCES

- [1] Z. Wang, H. R. Sheikh, and A. C. Bovik, "Objective video quality assessment," in *The Handbook of Video Databases: Design and Applications* (B. Furht and O. Marquie). Boca Raton, FL: CRC, 2003, pp. 1041–1078.
- [2] Y. Horita, S. Arata, and T. Murai, "No-reference image quality assessment for JPEG/JPEG2000 coding," in *Proc. EUSIPCO*, 2004, pp. 1301–1304.
- [3] R. Ferzli and L. J. Karam, "No-reference objective wavelet based noise immune image sharpness metric," in *Proc. IEEE Int. Conf. Image Processing*, Sep. 2005, vol. 1, pp. 405–408.
- [4] J. G. Robson and N. Graham, "Probability summation and regional variation in contrast sensitivity across the visual field," *Vis. Res.*, vol. 21, no. 3, pp. 409–418, 1981.
- [5] S. Erasmus and K. Smith, "An automatic focusing and astigmatism correction system for the SEM and CTEM," *J. Microscopy*, vol. 127, pp. 185–199, 1982.
- [6] C. F. Batten, "Autofocusing and Astigmatism Correction in the Scanning Electron Microscope," M.Phil. thesis, Univ. Cambridge, Cambridge, U.K., 2000.

- [7] P. Marziliano, F. Dufaux, S. Winkler, and T. Ebrahimi, "Perceptual blur and ringing metrics: Applications to JPEG2000," *Signal Process.: Image Commun.*, vol. 19, no. 2, pp. 163–172, Feb. 2004.
- [8] L. Firestone, K. Cook, N. Talsania, and K. Preston, "Comparison of autofocus methods for automated microscopy," *Cytometry*, vol. 12, pp. 195–206, 1991.
- [9] N. Zhang, A. Vladar, M. Postek, and B. Larabee, "A kurtosis-based statistical measure for two-dimensional processes and its application to image sharpness," in *Proc. Section of Physical and Engineering Sciences of American Statistical Society*, 2003, pp. 4730–4736.
- [10] J. Caviedes and F. Oberti, "A new sharpness metric based on local kurtosis, edge and energy information," *Signal Process.: Image Commun.*, vol. 19, no. 2, pp. 147–161, Feb. 2004.
- [11] N. K. Chern, N. P. A. Neow, and M. H. Ang, Jr, "Practical issues in pixel-based autofocusing for machine vision," in *Proc. IEEE Int. Conf. Robotics and Automation*, 2001, vol. 3, pp. 2791–2796.
- [12] X. Marichal, W. Ma, and H. J. Zhang, "Blur determination in the compressed domain using DCT information," in *Proc. IEEE Int. Conf. Image Processing*, Oct. 1999, vol. 2, pp. 386–390.
- [13] D. Shaked and I. Tastl, "Sharpness measure: Towards automatic image enhancement," in *Proc. IEEE Int. Conf. Image Processing*, Sep. 2005, vol. 1, pp. 937–940.
- [14] N. B. Nill and B. H. Bouzas, "Objective image quality measure derived from digital image power spectra," *Opt. Eng.*, vol. 31, no. 4, pp. 813–825, Nov. 1992.
- [15] J. J. DePalma and E. M. Lowry, "Sine wave response of the visual system ii: Sine wave and square wave contrast sensitivity," *J. Opt. Soc. Amer.*, vol. 52, no. 3, pp. 328–335, 1962.
- [16] J. A. Shagri, P. S. Cheatham, and A. Habibi, "Image quality based on human visual system model," *Opt. Eng.*, vol. 28, no. 7, pp. 813–818, 1986.
- [17] E. P. Ong, W. S. Lin, Z. K. Lu, S. S. Yao, X. K. Yang, and L. F. Jiang, "No-reference quality metric for measuring image blur," in *Proc. IEEE Int. Conf. Image Processing*, Sep. 2003, pp. 469–472.
- [18] I. BT.500-8, Methodology for the Subjective Assessment of the Quality of Television Pictures 1998.
- [19] N. Jayant, J. Johnston, and R. Safranek, "Signal compression based on models of human perception," *Proc. IEEE*, vol. 81, no. 10, pp. 1385–1422, 1993.
- [20] C. Poyton, *Digital Video and HDTV Algorithms and Interfaces*. San Francisco, CA: Morgan Kaufmann, 2003.
- [21] R. Ferzli and L. J. Karam, "Human visual system based on no-reference objective image sharpness metric," in *Proc. IEEE Int. Conf. Image Processing*, Oct. 2006, pp. 2949–2952.
- [22] L. V. Scharff, A. Hill, and A. J. Ahumada, "Discriminability measures for predicting readability of text on textured backgrounds," *Opt. Exp.*, vol. 6, pp. 81–91, Feb. 2000.
- [23] I. Hontsch and L. J. Karam, "Adaptive image coding with perceptual distortion control," *IEEE Trans. Image Process.*, vol. 11, no. 3, pp. 213–222, Mar. 2002.
- [24] Z. Liu, L. J. Karam, and A. B. Watson, "JPEG2000 encoding with perceptual distortion control," *IEEE Trans. Image Process.*, vol. 15, no. 7, pp. 1763–1778, Jul. 2006.
- [25] G. Wang, T.-T. Wong, and P.-A. Heng, "Deringing cartoons by image analogies," *ACM Trans. Graph.*, vol. 25, no. 4, pp. 1360–1379, Oct. 2006.
- [26] H. R. Sheikh, A. C. Bovik, L. Cormack, and Z. Wang, LIVE Image Quality Assessment Database 2003 [Online]. Available: <http://live.ece.utexas.edu/research/quality>
- [27] VQEG, Final Report From the Video Quality Experts Group on the Validation of Objective Models of Video Quality Assessment, Mar. 2000 [Online]. Available: <http://www.vqeg.org/>
- [28] D. Freedman, R. Pisani, and R. Purves, *Statistics*, 3rd ed. New York: W. W. Norton, 1997.



**Rony Ferzli** received the B.E. and M.E. degrees in electrical engineering from the American University of Beirut, Lebanon, in 1999 and 2002, respectively. He received the Ph.D. degree in electrical engineering from Arizona State University (ASU), Tempe, in 2007, researching image quality assessment.

He is currently working in the R&D Unified Communications Group at Microsoft Corp., Redmond, WA, designing next generation video codecs for video conferencing products. His research interests are in image and video processing, computer vision, DSP architectures and real-time systems, neural networks, and mixed-signal design.



**Lina J. Karam** (SM'91–M'95–SM'03) received the B.E. degree in computer and communications engineering from the American University of Beirut, Lebanon, in 1989, and the M.S. and Ph.D. degrees in electrical engineering from the Georgia Institute of Technology (Georgia Tech), Atlanta, in 1992 and 1995, respectively.

She is currently an Associate Professor in the Electrical Engineering Department, Arizona State University, Tempe. Her research interests are in the areas of image and video processing, image and video coding, visual quality assessment, human perception, error-resilient source coding, medical imaging, and digital filtering. From 1991 to 1995, she was a graduate research assistant in the Graphics, Visualization, and Usability (GVU) Center and then in the Department of Electrical Engineering, Georgia Tech. She worked at Schlumberger Well Services on problems related to data modeling and visualization, and in the Signal Processing Department of AT&T Bell Labs on problems in video coding during 1992 and 1994, respectively.

Prof. Karam is a recipient of an NSF CAREER Award. She served as the Chair of the IEEE Communications and Signal Processing Chapters in Phoenix, AZ, in 1997 and 1998. She also served as an Associate Editor of the IEEE TRANSACTIONS ON IMAGE PROCESSING from 1999 to 2003 and of the IEEE SIGNAL PROCESSING LETTERS from 2004 to 2006, and as a member of the IEEE Signal Processing Society's Conference Board from 2003 to 2005. She is currently serving as an Associate Editor of the IEEE TRANSACTIONS ON IMAGE PROCESSING and as the Technical Program Chair of the 2009 IEEE International Conference on Image Processing. She is an elected member of the IEEE Circuits and Systems Society's DSP Technical Committee, the IEEE Signal Processing Society's IMDSP Technical Committee, and a member of the editorial board of the *Foundation Trends in Signal Processing* journal. She is a member of the Signal Processing, and Circuits and Systems societies of the IEEE.